N96-15601

RADIANT EXTINCTION OF GASEOUS DIFFUSION FLAMES

Arvind Atreya, Sanjay Agrawal, Tariq Shamim & Kent Pickett
University of Michigan; Ann Arbor, MI 48109

Kurt R. Sacksteder
NASA Lewis Research Center; Cleveland, OH 44135

Howard R. Baum
NIST, Gaithersburg, MD 20899

INTRODUCTION

The absence of buoyancy-induced flows in microgravity significantly alters the fundamentals of many combustion processes. Substantial differences between normal-gravity and microgravity flames have been reported during droplet combustion[1], flame spread over solids[2,3], candle flames[4] and others. These differences are more basic than just in the visible flame shape. Longer residence time and higher concentration of combustion products create a thermochemical environment which changes the flame chemistry. Processes such as flame radiation, that are often ignored under normal gravity, become very important and sometimes even controlling. This is particularly true for conditions at extinction of a μg diffusion flame.

Under normal-gravity, the buoyant flow, which may be characterized by the strain rate, assists the diffusion process to transport the fuel & oxidizer to the combustion zone and remove the hot combustion products from it. These are essential functions for the survival of the flame which needs fuel & oxidizer. Thus, as the strain rate is increased, the diffusion flame which is "weak" (reduced burning rate per unit flame area) at low strain rates is initially "strengthened" and eventually it may be "blown-out." Most of the previous research on diffusion flame extinction has been conducted at the high strain rate "blow-off" limit. The literature substantially lacks information on low strain rate, radiation-induced, extinction of diffusion flames. At the low strain rates encountered in μg, flame radiation is enhanced due to: (i) build-up of combustion products in the flame zone which increases the gas radiation, and (ii) low strain rates provide sufficient residence time for substantial amounts of soot to form which further increases the flame radiation. It is expected that this radiative heat loss will extinguish the already "weak" diffusion flame under certain conditions. Identifying these conditions (ambient atmosphere, fuel flow rate, fuel type, etc.) is important for spacecraft fire safety. Thus, the objective of this research is to experimentally and theoretically investigate the radiation-induced extinction of diffusion flames in μg and determine the effect of flame radiation on the "weak" μg diffusion flame.

RESEARCH APPROACH

To investigate radiation-induced extinction, spherical and counterflow geometries are chosen for μg & *1-g* respectively for the following reasons: Under μg conditions, a spherical burner is used to

produce a spherical diffusion flame. This forces the combustion products (including soot which is formed on the fuel side of the diffusion flame) into the high temperature reaction zone and may cause radiative-extinction under suitable conditions. Under normal-gravity conditions, however, the buoyancy-induced flow field around the spherical burner is complex and unsuitable for studying flame extinction. Thus, a one-dimensional counterflow diffusion flame is chosen for *1-g* experiments and modeling. At low strain rates, with the diffusion flame on the fuel side of the stagnation plane, conditions similar to the μg case are created -- the soot is again forced through the high temperature reaction zone. The *1-g* experiments are primarily used to determine the rates of formation and oxidation of soot in the thermochemical environment present under μg conditions. These rates are necessary for modeling purposes. Transient numerical models for both μg and *1-g* cases are being developed to provide a theoretical basis for the experiments. These models include soot formation and oxidation and flame radiation and will help quantify the low-strain-rate radiation-affected diffusion flame extinction limits.

RESULTS

Significant progress has been made on both experimental and theoretical parts of this research. This may be summarized as follows:

1) Experimental and theoretical work on determining the expansion rate of the μg spherical diffusion flame. Preliminary results were presented at the AIAA conference (Ref. 5).
2) Theoretical modeling of zero strain rate transient diffusion flame with radiation (Ref. 6).
3) Experimental and theoretical work for determining the radiation from the μg spherical diffusion flame. Preliminary results were presented at the AIAA conference (Ref. 7).
4) Theoretical modeling of finite strain rate transient counterflow diffusion flame with radiation (Ref 8).
5) Experimental work on counterflow diffusion flames to determine the soot formation and oxidation rates (Ref. 9).

The above experimental and theoretical work is briefly summarized in the remainder of this section.

Experimental Work: The μg experiments were conducted in the 2.2 sec drop tower at the NASA Lewis Research Center and the counterflow diffusion flame experiments (not described here) were performed at UM. For the μg experiments, a porous spherical burner was used to produce nearly spherical diffusion flames. Several experiments, under ambient pressure and oxygen concentration conditions, were performed with methane (less sooty), ethylene (sooty), and acetylene (very sooty) for flow rates ranging from 4 to 28 cm^3/s. These fuel flow rates were set by a needle valve and a solenoid valve was used to open and close the gas line to the burner upon computer command. Two ignition methods were used for these experiments: (i) The burner was ignited in *1-g* with the desired fuel flow rate and the package was dropped within one second after ignition. (ii) The burner was ignited in *1-g* with a very low flow rate of H_2 and the flow was switched to the desired flow rate of the given fuel in μg just after the commencement of the drop. Following measurements were made during the μg experiments:

i) The *flame radius* was measured from photographs taken by a color CCD camera. Image processing was used to determine both the flame radius and the relative image intensity. Sample photographs are shown in Photos E1 to E3 for ethylene and A1 to A3 for acetylene.
ii) The *flame radiation* was measured by the three photodiodes with different spectral absorptivities. The first photodiode essentially measures the blue & green radiation, the second photodiode captures the yellow, red & near infra-red radiation, and the third photodiode is for infra-red radiation from 0.8 to 1.8 μm.
iii) The *flame temperature* was measured by two S-type thermocouples and the sphere surface temperature was measured by a K-type thermocouple. In both cases 0.003" diameter wire was used. The measured temperatures were later corrected for time response and radiation.

It is interesting to note that for both ethylene and acetylene (see the progressive flame growth in the Color Photos) initially the flame is blue (non-sooty) but becomes bright yellow (sooty) under μg conditions. Later, as the *μg* time progresses, the flame grows in size and becomes orange and less luminous and the soot luminosity seems to disappear. A possible explanation for this observed behavior is suggested by the theoretical calculations of Ref. 6 & 8. The soot volume fraction first quickly increases and later decreases as the local concentration of combustion products increases. Essentially, further soot formation is inhibited by the increase in the local concentration of the combustion products and soot oxidation is enhanced [Ref.9,10]. Also, the high temperature reaction zone moves away from the already present soot leaving behind a relatively cold (non-luminous) soot shell. (A soot-shell is clearly visible in the ethylene Photo E2.) Thus, at the onset of μg conditions, initially a lot of soot is formed in the vicinity of the flame front (the outer faint blue envelope in the photographs) resulting in bright yellow emission. As the flame grows, several events reduce the flame luminosity: (i) The high concentration of combustion products left behind by the flame front inhibits the formation of new soot and promotes soot oxidation. (ii) The primary reaction zone, seeking oxygen, moves away from the soot region and the soot is pushed toward cooler regions by thermophoresis. Both these effects increase the distance between the soot layer and the reaction zone. (iii) The dilution and radiative heat losses caused by the increase in the concentration of the combustion products reduces the flame temperature which in turn reduces the soot formation rate and the flame luminosity.

Upon further observation, we note that the ethylene flames become blue toward the end of the *μg* time while the acetylene flames remain luminous yellow (although the intensity is significantly reduced as seen by the photodiode measurements in Figure 2). This is because of the higher sooting tendency of acetylene which enables soot formation to persist for a longer time. Thus, acetylene soot remains closer to the high temperature reaction zone for a longer time making the average soot temperature higher and the distance between the soot and the reaction layers smaller. Eventually, as is evident from Figure 2, even the acetylene flames will become blue in *μg*. From Figure 2 we note that the peak radiation intensity occurs at about 2.5 cm flame radius which corresponds to a time of about 0.2 seconds. This is almost the location of the first thermocouple whose output is plotted in Figures 3 & 4 as Tgas(1). From the temperature measurements presented in Figures 3 & 4, we note that: (i) The flame radiation significantly reduces the flame temperature (compare the peaks of the second thermocouple with those of the first for both fuels) by approximately 300K for ethylene and 500K for acetylene. (In fact, the acetylene flame seems to be on the threshold of extinction at this instant.) (ii) The temperature of the acetylene flame is about 200K lower than the ethylene flame at the first thermocouple location. (iii) The final gas temperature is also about 100K lower for the acetylene flame, which is consistent with larger radiative heat loss.

The data from the photodiodes is further reduced to obtain the total soot mass and the average temperature of the soot layer. This is plotted in Figures 5 & 6. These figures show that the average acetylene soot layer temperature is higher than the average ethylene soot layer temperature. The total soot mass produced by acetylene peaks at 0.2 seconds which corresponds to the peak of the first thermocouple, explaining the large drop in temperature. Also, the acetylene soot layer is cooling more slowly than the ethylene soot layer which is consistent with the above discussion regarding the photographic observations. Thus, for ethylene the reaction layer is moving away faster from the soot layer than in the case of acetylene. This is also consistent with the fact that ethylene soot mass becomes nearly constant but the acetylene soot mass reduces due to oxidation. Finally, the rate of increase in the total soot mass (i.e. the soot production rate) should be related to the sooting tendency of a given fuel. This corresponds to the slope of the soot mass curve in Figures 5 & 6. Clearly, the slope for acetylene is higher.

The flame radius measurements, presented in Figure 1, show a substantial change in the growth rate from initially being roughly proportional to $t^{1/2}$ to eventually (after significant radiative heat loss) being

proportional to $t^{1/5}$. In Ref. 5, we had developed a model for the expansion rate of non-radiating flames which is currently being modified to include the effects of radiant heat loss.

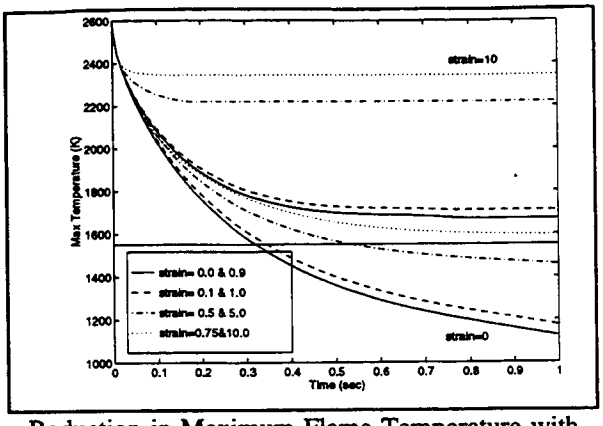

Reduction in Maximum Flame Temperature with Radiation (T_∞=295K, $Y_{F\infty}$=0.125, $Y_{O\infty}$=0.5)

Theoretical Work: Due to lack of space, only our most recent theoretical work is summarized here. In this work, to quantify the low-strain-rate radiation-induced diffusion flame extinction limits, a computational model has been developed for an unsteady counterflow diffusion flame. So far, only the radiative heat loss from combustion products (CO_2 and H_2O) have been considered in the formulation. The computations show a significant reduction in the flame temperature due to radiation. The adjacent figure shows the time variations of the maximum flame temperature for various values of the strain rates. This plot shows that for flames with strain rates less than 1 s^{-1}, the effect of gas radiation is sufficient to cause extinction. These results agree with our earlier study [6] at zero strain rate where gas radiation was also found to be sufficient to cause extinction. Clearly, additional radiation due to soot will extinguish the flames at higher strain rates.

Acknowledgements: This project is supported by NASA under contract no. NAG3-1460.

REFERENCES

1. *Jackson, G., S., Avedisian, C., T. and Yang, J., C.*, Int. J. Heat Mass Transfer., Vol.35, No. 8, pp. 2017-2033, 1992.

2. *T'ien, J. S., Sacksteder, K. R., Ferkul, P. V. and Grayson, G. D.* "Combustion of Solid Fuels in very Low Speed Oxygen Streams," Second International Microgravity Combustion Workshop," NASA Conference Publication, 1992.

3. *Ferkul, P., V.*, "A Model of Concurrent Flow Flame Spread Over a Thin Solid Fuel," NASA Contractor Report 191111, 1993.

4. *Ross, H. D., Sotos, R. G. and T'ien, J. S.*, Combustion Science and Technology, Vol. 75, pp. 155-160, 1991.

5. *Atreya, A, Agrawal, S., Sacksteder, K., and Baum, H.*, "Observations of Methane and Ethylene Diffusion Flames Stabilized around a Blowing Porous Sphere under Microgravity Conditions," AIAA paper # 94-0572, January 1994.

6. *Atreya, A. and Agrawal, S.*, "Effect of Radiative Heat Loss on Diffusion Flames in Quiescent Microgravity Atmosphere," Accepted for publication in Combustion and Flame, 1993.

7. *Pickett, K., Atreya, A., Agrawal, S., and Sacksteder, K.*, "Radiation from Unsteady Spherical Diffusion Flames in Microgravity," AIAA paper # 95-0148, January 1995.

8. *Shamim, T., and Atreya, A.* "A Study of the Effects of Radiation on Transient Extinction of Strained Diffusion Flames," Central States Combustion Institute Meeting, 1995.

9. *Atreya, A. and Zhang, C.*, "A Global Model of Soot Formation derived from Experiments on Methane Counterflow Diffusion Flames," in preparation for submission to Combustion and Flame.

10. *Zhang, C., Atreya, A. and Lee, K.*, Twenty-Fourth (International) Symposium on Combustion, The Combustion Institute, pp. 1049-1057, 1992.

11. *Atreya, A.*, "Formation and Oxidation of Soot in Diffusion Flames," Annual Technical Report, GRI-91/0196, Gas Research Institute, November, 1991.

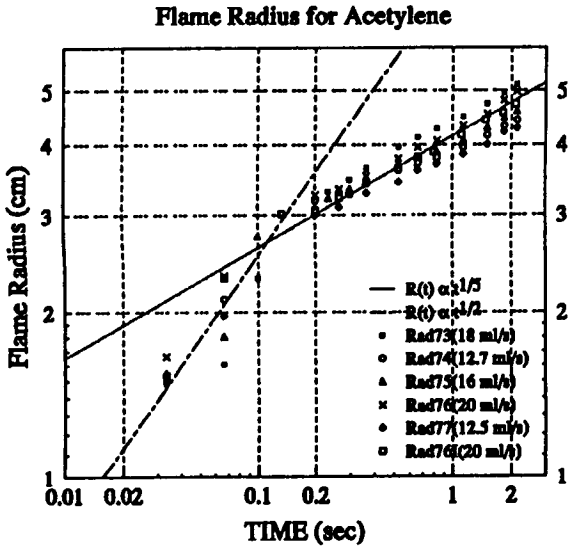

Figure 1

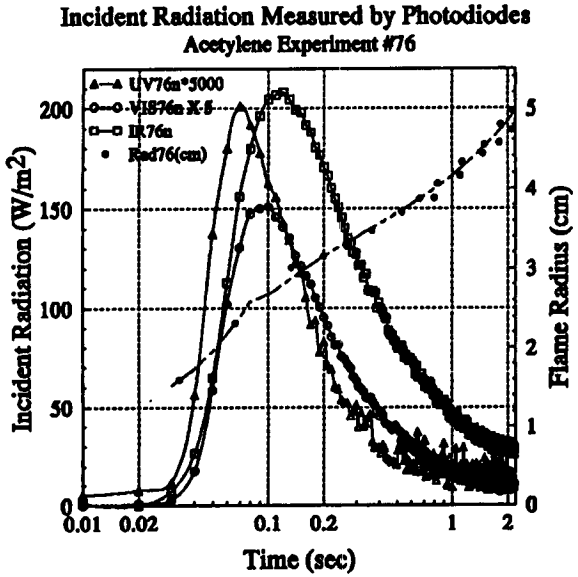

Figure 2

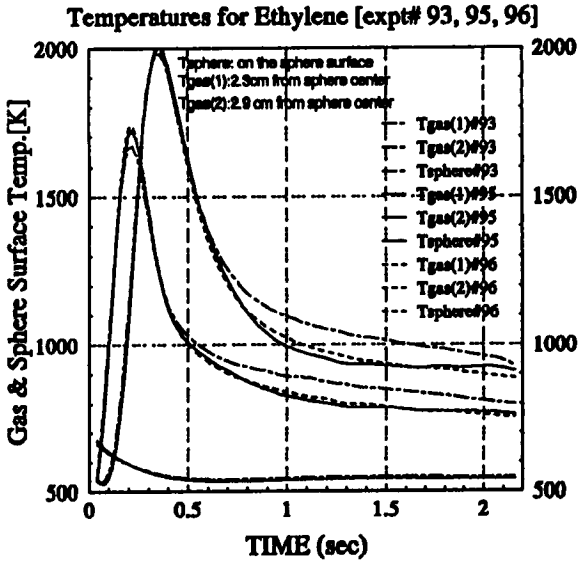

Figure 3

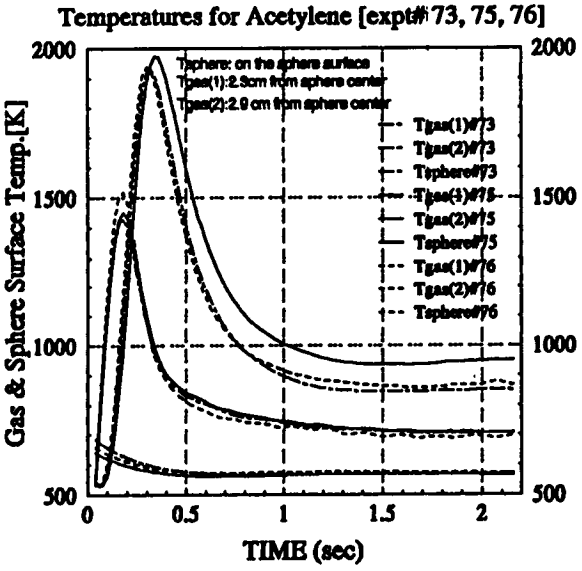

Figure 4

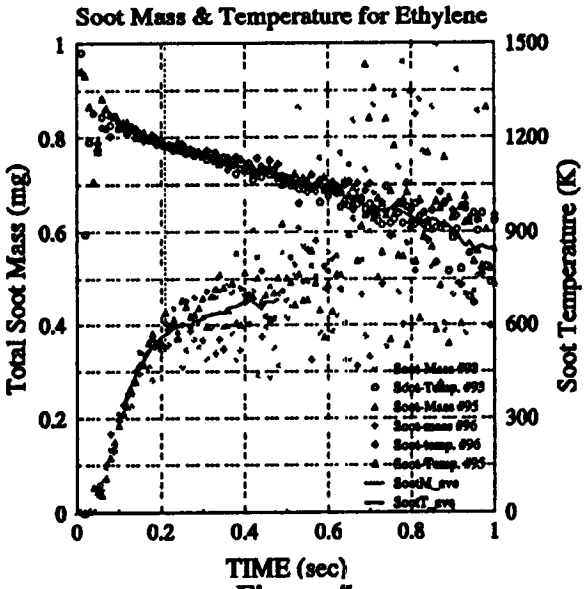

Figure 5

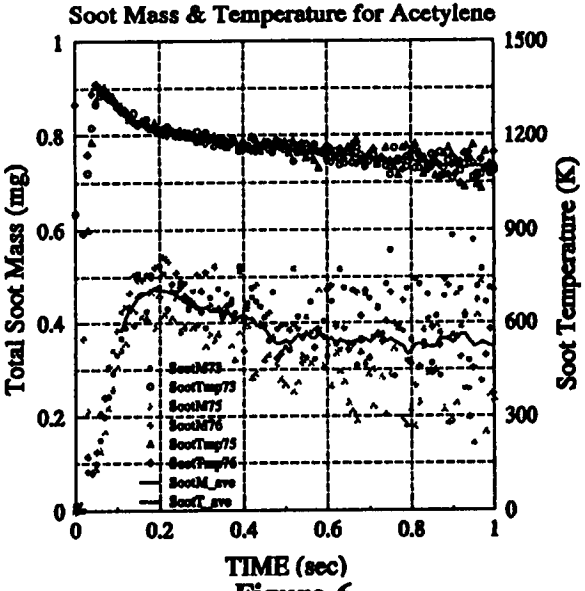

Figure 6

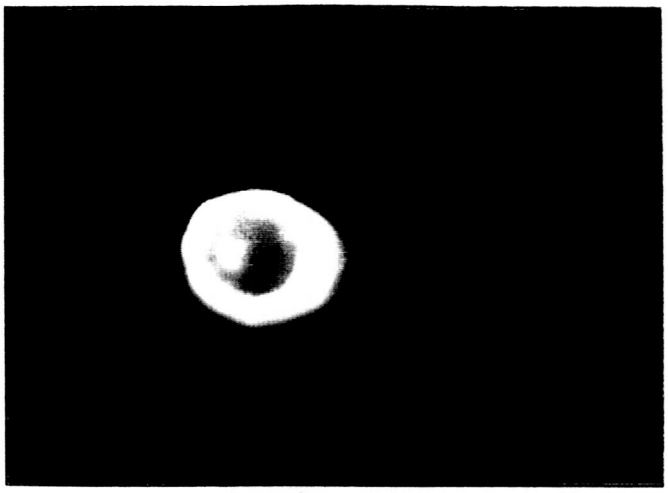

Photo E1. Ethylene flame at 0.067 sec μg time. (Flow rate: 20 ml/sec)

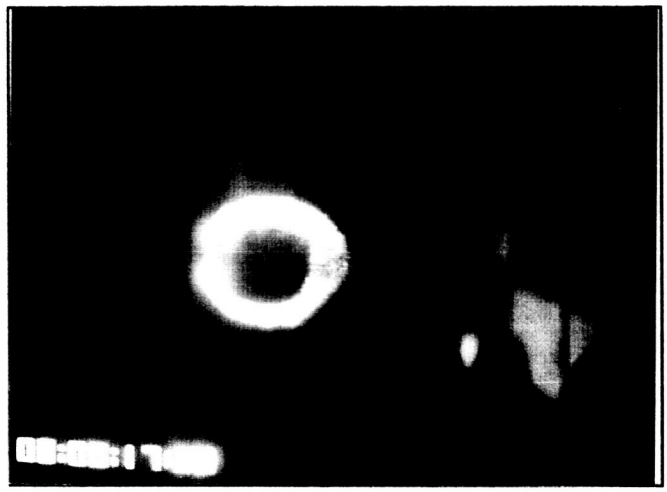

Photo A1. Acetylene flame at 0.067 sec μg time. (Flow rate: 20 ml/sec)

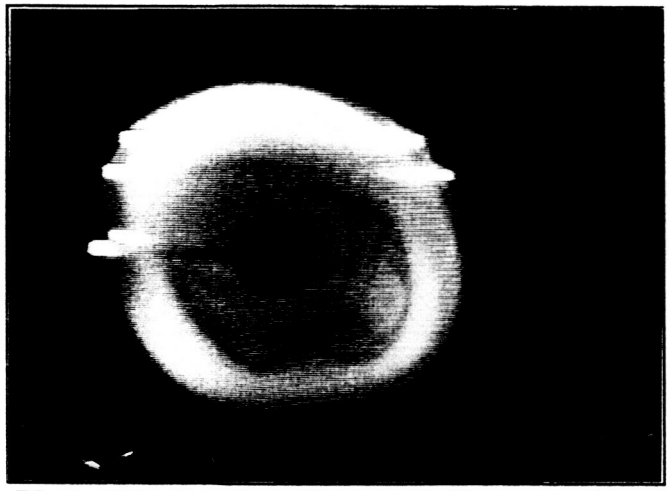

Photo E2. Ethylene flame at 1.37 sec μg time. (Flow rate: 20 ml/sec)

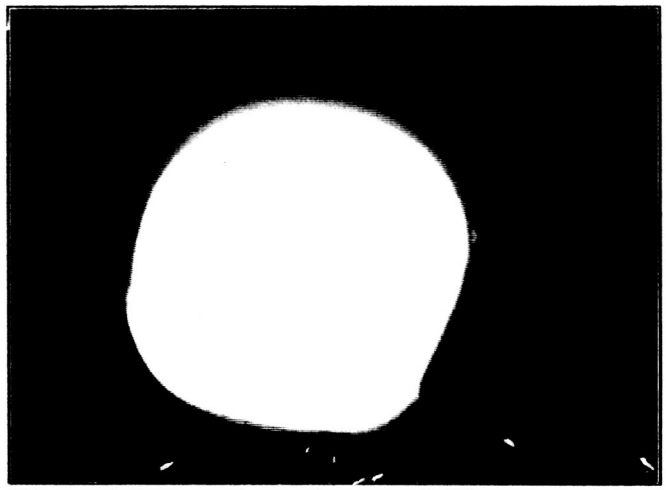

Photo A2. Acetylene flame at 0.50 sec μg time. (Flow rate: 20 ml/sec)

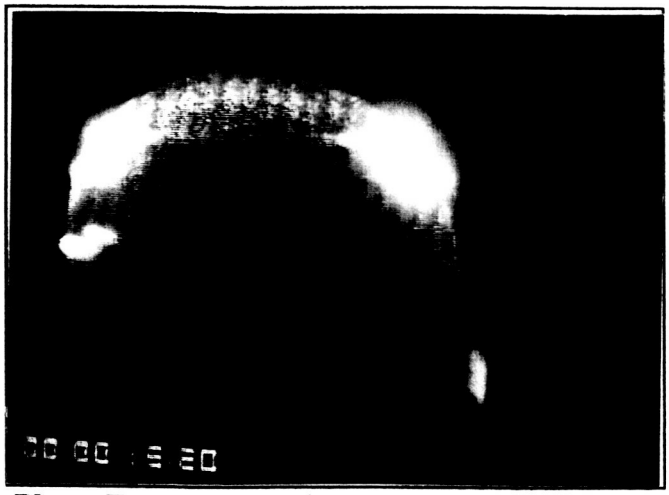

Photo E3. Ethylene flame at 1.80 sec μg time. (Flow rate: 20 ml/sec)

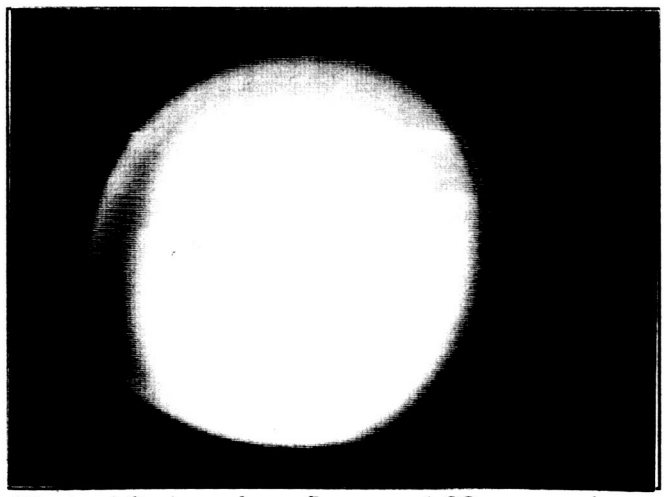

Photo A3. Acetylene flame at 1.90 sec μg time. (Flow rate: 20 ml/sec)